Highly Crosslinked Nanocomposites of Aromatic Dicyanates/SiO_2 via the Sol–Gel Method

Rong-Hsien Lin,[1] Chih-Wei Lin,[2] An-Cheng Lee,[1] Yi-Hung Chen,[1] Fu-Shan Yen[1]

[1]*Department of Chemical and Material Engineering, National Kaohsiung University of Applied Sciences, Kaohsiung 80782, Taiwan*
[2]*Department of Materials Science and Engineering, National Tsing Hua University, Hsinchu 30013, Taiwan*

Received 13 June 2006; accepted 18 July 2006
DOI 10.1002/app.25433
Published online in Wiley InterScience (www.interscience.wiley.com).

ABSTRACT: Highly crosslinked nanocomposites of bisphenol A dicyanate (BADCy) containing silica clusters were successfully prepared via the sol–gel process. The silica clusters were generated from various metal alkoxide precursors, including methyltrimethoxysilane (TMOS), 3-glycidoxypropyltrimethoxysilane (GPOS), and 2-(3,4-epoxycyclohexyl) ethyltrimethoxysilane (ECOS). The metal alkoxide precursors GPOS and ECOS were, in turn, used as coupling agents. Three kinds of systems involving BADCy/TMOS, BADCy/coupling agent, and BADCy/TMOS/coupling agent were individually prepared and thoroughly investigated using various methods. Each kind of system was of a particular characterization and morphology and had distinct physical and dielectric properties. Isolated silica clusters on a nanoscale were homogenously distributed in the highly crosslinked BADCy/TMOS hybrid system. The characterization of BADCy/TMOS nanocomposites showed improved physical properties, when compared with the neat BADCy network. The particle sizes can be controlled by adding different amounts of TMOS and are slightly increased (in the range of 50–105 nm) with increasing TMOS content. On the other hand, in the highly crosslinked BADCy/coupling agent hybrid system, the silica clusters were tethered to the BADCy matrix by the coupling agent. An oxazoline linkage was detected during the reaction of cyanate groups in BADCy with the epoxide groups in the coupling agent. These nanocomposites exhibited weakened mechanical properties but are of a smaller and more homogenous particle size in the range of 30–50 nm, irrespective of the silica content. Finally, the BADCy/TMOS/coupling agent system was successfully designed to combine the advantages of the two systems mentioned above. J Appl Polym Sci 103: 1356–1366, 2007

Key words: crosslinking; nanocomposites; aromatic dicyanates; sol–gel; thermosets

INTRODUCTION

In recent years, organic/inorganic hybrid nanocomposites have been extensively researched, because these hybrids were used for blending inorganic fillers and organic polymers on a molecular scale, combining the advantages of each component. These materials can be formed via several different approaches. One successful approach has been the *in situ* polymerization of metal alkoxide precursors in polymer matrices via the sol–gel method. This method involves the hydrolysis of metal alkoxides to produce metal hydroxides, followed by the condensation of hydroxyl groups to form inorganic clusters.[1] When inorganic clusters are mixed with polymer solutions or with monomers for polymerization, organic/inorganic hybrid nanocomposites can be obtained. A lot of thermoplastics have been considered for the preparation of organic/inorganic nanocomposites by the sol–gel process, such as PS/SiO_2,[2] polyimide/SiO_2,[3–8] PMMA/SiO_2,[9–12] PEK/SiO_2,[13] polyimide/TiO_2,[14,15] Nafion®/ SiO_2,[16] etc. Only a few researchers have studied thermosetting systems and have primarily focused on epoxy resins.[17–20]

Cyanate ester resins are one of the most important thermosetting polymers because of their high thermal stability, excellent mechanical and electronical properties.[21] Thus, they have been used in high performance electronic devices and aerospace applications. Various aromatic dicyanates were substantially investigated in our laboratory on the cure kinetics and mechanisms of polycyclotrimerization,[22–24] the glass transition temperature-conversion relationship in the polycyclotrimerization,[25,26] and the cure reaction of bismaleimide (BMI)/bisphenol A dicyanate (BADCy) blend.[23,27,28] Pyrimidine and/or pyridine linkage structures were found during the crosslinking reactions in this blend. In another study, the cure reactions of liquid aromatic dicyanate ester (1,1′-bis(4-cyanatophenyl) ethane, DiCy) with different types of epoxy resins were also investigated.[29] In the curing system of DiCy associated with bisphenol A epoxide, both oxazoline and oxazolidinone linkages were observed after being completely cured, whereas in the curing system of DiCy associated with a liquid cycloaliphatic epoxy ester (3,4-epoxycy-

Correspondence to: R.-H. Lin (rongh@cc.kuas.edu.tw).
Contract grant sponsor: National Science Council; contract grant number: NSC 93-2216-E-151-002.

clohexylmethyl-3,4-epoxycyclohexane-carboxylate), only oxazoline linkage was detected.

The objectives of this work were to develop a highly crosslinked nanocomposite of aromatic dicyanates/SiO_2 by the sol–gel method. Characterization and properties of the nanocomposites were thoroughly investigated. To improve the compatibility between the organic and inorganic phases, the coupling agents with an epoxide group on one end and alkoxysilyl group on the other end were used. Cross-reaction was expected between the epoxide group of the coupling agent and the cyanate group of the matrix in a reaction similar to the previously stated one. The end result with metal alkoxides in the coupling agent may be the source of poly(silsesquioxanes) (POSS). Furthermore, the effects of the coupling agent on the size of the SiO_2 particles and the properties were also studied.

EXPERIMENTAL

Materials

Bisphenol A dicyanate (BADCy; TCI, Japan), methyltrimethoxysilane (TMOS; Aldrich Chemicals), 3-glycidoxypropyltrimethoxysilane (GPOS; Aldrich Chemicals), and 2-(3,4-epoxycyclohexyl) ethyltrimethoxysilane (ECOS; Fluka, Switzerland) were used as purchased. BADCy underwent polycyclotrimerization and served as the matrix component. TMOS was used as the precursor of inorganic clusters of SiO_2. GPOS or ECOS acted as coupling agents. The chemical structures of BADCy, TMOS, ECOS, and GPOS are as follows:

BADCy :

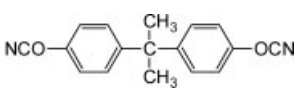

TMOS :

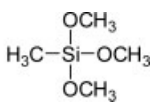

ECOS :

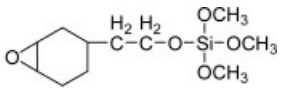

GPOS :

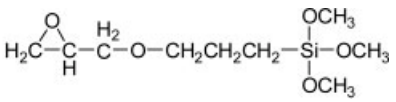

Preparation of cyanate ester/SiO_2 hybrids

Before the cyanate ester/SiO_2 hybrid nanocomposites were fabricated, the two solutions A and B were prepared individually. Solution A was prepared by dissolving the BADCy monomer in a THF solvent. Solution B was composed of TMOS (or ECOS, or GPOS)/H_2O/HCl/THF in a specified mole ratio. In the first step, TMOS, ECOS, or GPOS was precisely weighed in and mixed with pure water in a mole ratio of 2 : 1 (water/TMOS), and was then poured into the THF solvent. An appropriate amount of HCl was used to adjust the pH value of Solution B to the level of 2. Meanwhile, HCl might act as a catalyst for the hydrolysis of metal alkoxides (TMOS, ECOS, or GPOS). Solution B was stirred at room temperature for 30 min, so that it underwent the hydrolysis and condensation reactions. Appropriately sized nanoparticles were thus obtained. Subsequently, Solutions A and B were thoroughly mixed and stirred for another hour to carry out the hydrolysis and condensation reactions further. Finally, the resulting solution was cast upon an aluminum dish, dried in a vacuum oven, and thermally treated at progressively ascending temperatures of 80°C, 120°C, and 180°C for 1 h, then 230°C and 250°C for 2 h, respectively. The cyanate ester/SiO_2 hybrid nanocomposites were thus obtained.

Instrumentation

(1) Differential scanning calorimetry (DSC): Samples approximately 3–6 mg in weight were sealed in hermetic pans and were scanned in a differential scanning calorimeter (Perkin–Elmer DSC-7) calibrated with an indium standard. A stream of nitrogen at a flow rate of 20 mL/min was used to purge the DSC cell. (2) Fourier-transform infrared (FTIR) spectra were recorded on a Digi-Lab FTS-40 FTIR spectrometer. The samples were mixed with dried KBr powder and were pressed into pellets. Spectra were obtained in an optical range of 400–4000 cm^{-1} by averaging 32 scans at a resolution of 8 cm^{-1}. (3) The molecular structures of the synthesized poly(silsesquioxanes) (POSS) precursors were characterized by solid state ^{29}Si NMR (Bruker Avance 400 NMR spectrometer). (4) Particle size analysis of POSS precursors was conducted in a Brookhaven 90plus particle size analyzer before addition to the matrix. (5) The morphology of the fracture surfaces of the hybrid was observed with a JEOL 5610 scanning electron microscope (SEM). (6) The thermal properties were determined with a TA instrument, TGA 2960, at a heating rate of 20°C/min under nitrogen atmosphere. The temperature range for the TGA measurements was from 50 to 800°C. (7) Dynamic mechanical analysis (storage E' and loss (tan δ)) was performed over a temperature range of 50–350°C with a Perkin–Elmer DMA-7 at a heating rate of 5°C/min and at 1-Hz frequency; a thickness of $\sim$ 30 μm was used for measurement. The temperature was calibrated with an indium standard. A stream of nitrogen at a flow rate of 30 mL/min was used to purge the DMA cell. (8) Dielectric

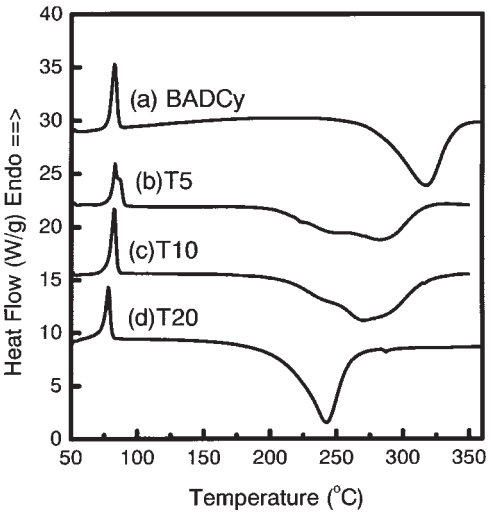

Figure 1 DSC thermograms at a heating rate of 20°C/min; (a) neat BADCy, (b) with 5 phr TMOS (T5), (c) with 10 phr TMOS (T10), and (d) with 20 phr TMOS (T20).

constants were measured by an impedance analyzer (HP4291B) coupled with HP16453A instrument at frequencies of 1.8 GHz and 1 GHz.

RESULTS AND DISCUSSIONS

Before the nanocomposite systems were investigated, the cure reaction of neat BADCy was preliminarily examined through a cross-reference between FTIR spectra and DSC thermograms. Figure 1(a) shows the DSC thermogram of the neat BADCy at a heating rate of 20°C/min. Only one exothermic peak was observed in the DSC trace over the temperature range of 240–360°C, suggesting that a cure reaction took place during the thermal treatment. Correspondingly, the FTIR spectra were measured to analyze the cure reaction of BADCy. Shown in Figures 2(a) and (b) are the FTIR spectra of the BADCy monomer and the completely cured BADCy, respectively. Comparing the difference of both spectra, the disappearing absorption bands of the cyanate at 2267 and 2237 cm^{-1} were accompanied with the emerging absorption of triazine (1565 and 1366 cm^{-1}). This suggests that polycyclotrimerization is the exclusive reaction in the system and only one type of linkage is formed during the whole course of the reaction. Polycyclotrimerization of aromatic dicyanates proceeds via a combination of three functional groups to form a triazine ring, illustrated as Path 1 in Scheme 1, thereby forming a highly crosslinked network.

BADCy/TMOS nanocomposite system

Characterization of hybrid in the cure reactions

Shown in Figures 1(b–d) are the DSC thermograms of curing the BADCy hybrid associated with different levels of TMOS content (5, 10, and 20 phr), respectively. DSC traces for sample T5 (5 phr TMOS) and T10 (10 phr TMOS) show a main exothermic peak accompanied by a shoulder peak in the lower temperature region. The main exothermic peak shifts to a lower temperature, when compared with that of neat BADCy [Fig. 1(a)], suggesting that the BADCy component was induced to undergo a reaction in the presence of residual acid and hydrolyzed —OH groups in the hybrid.[22–24] Acid or the —OH group acts as a catalyst in the polycyclotrimerization of dicyanate esters. The higher the content of TMOS (hydrolyzed to form —OH groups), the further towards lower temperatures the shift occurs, and eventually, the main peak merges in the shoulder

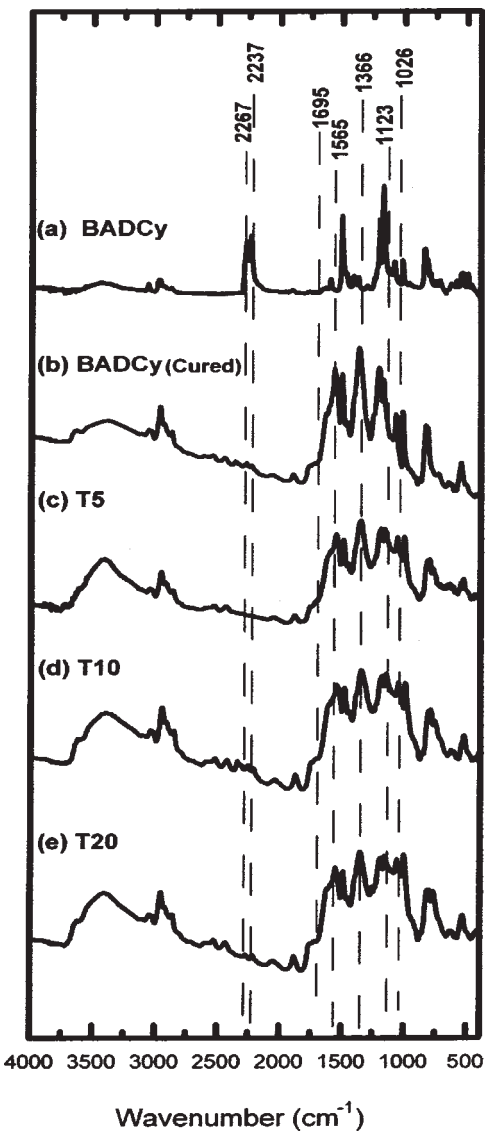

Figure 2 FTIR spectra for (a) neat BADCy monomer, (b) cured BADCy, (c) cured T5 (with 5 phr TMOS), (d) cured T10 (with 10 phr TMOS), and (e) cured T20 (with 20 phr TMOS).

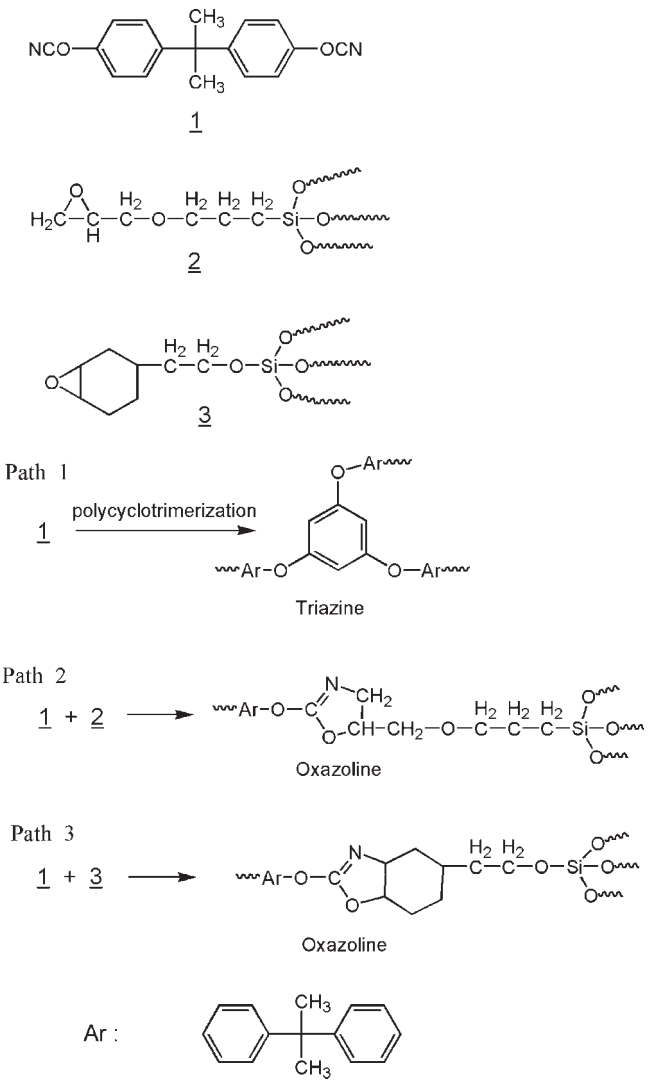

Scheme 1 Scheme for reactions; Path (1) polycyclotrimerization of dicyanate ester (BADCy); Path (2) reaction of BADCy with GPOS; and Path (3) reaction of BADCy with ECOS.

peak, as shown in Figure 1(d) (T20; 20 phr TMOS). The shoulder peak is supposedly attributed to the further condensation of the silica cluster (POSS) during the cure reaction, which was demonstrated by the SEM images in the following section by the slight growth of the silica cluster observed during the cure reaction.

The corresponding FTIR spectra for the cured BADCy/SiO_2 hybrids are shown in Figures 2(c–e), respectively. The characteristic absorption peaks of the triazine at 1565 and 1366 cm^{-1} were observed in all the cured samples (T5, T10, and T20), suggesting that polycyclotrimerization of the dicyanate ester proceeds, and the highly crosslinked hybrids were thus fabricated. Besides, the characteristic absorption bands of the hydrolysis and condensation products of TMOS were also observed. The spectra show absorption bands for Si—OH stretching at 3440 and 843 cm^{-1}, and the broadened Si—O—Si absorption bands at 1123 and 1026 cm^{-1}, which can be assigned to the cage and network structures of POSS, respectively.[30,31]

The molecular structures of the synthesized POSS precursors were characterized by a solid state ^{29}Si NMR, and these are affected by the factors of water content, reaction time, and curing temperature.[17,30] For TMOS, mono-, di-, and trisubstituted siloxane bonds are designated as T^1, T^2, and T^3, respectively. Figure 3(a) displays the solid-state ^{29}Si NMR spectrum of the cured nanocomposite sample T5. Chemical shifts of −57 and −66 ppm were detected, and assigned to T^2 and T^3, respectively. The solid-state ^{29}Si NMR spectrum for samples T10 and T20 are not shown here for brevity. All results showed that T^3 was the predominant microstructure, revealing that most of the TMOS formed a network or cage structure. This is comparable to the results of the FTIR spectra.

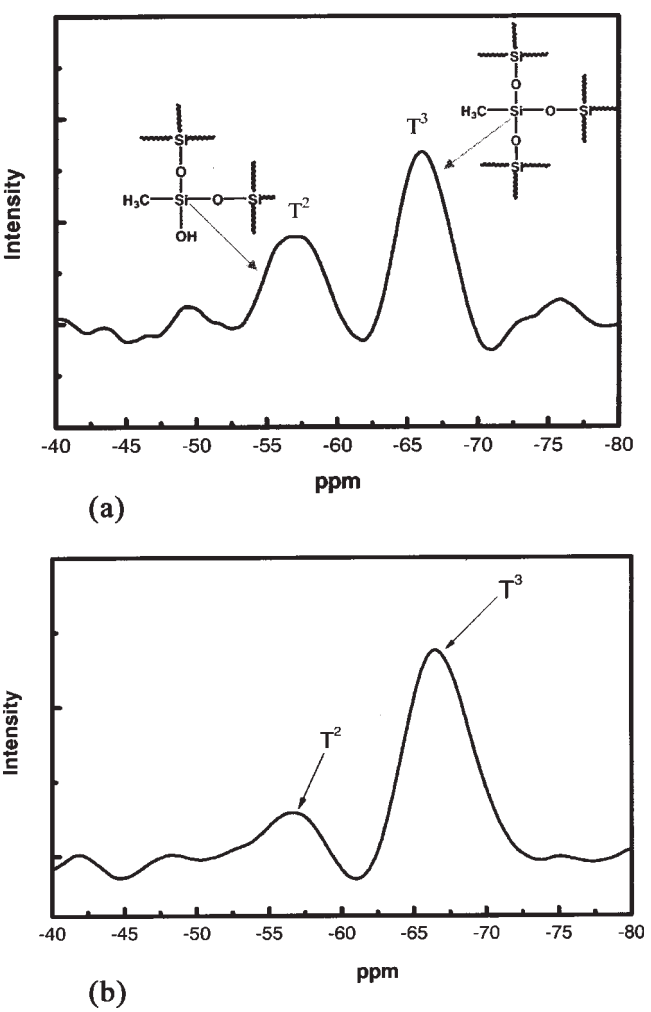

Figure 3 Solid-state ^{29}Si NMR spectrum for (a) cured nanocomposite sample T5 (with 5 phr TMOS), and (b) cured nanocomposite sample E20 (with 20 phr ECOS).

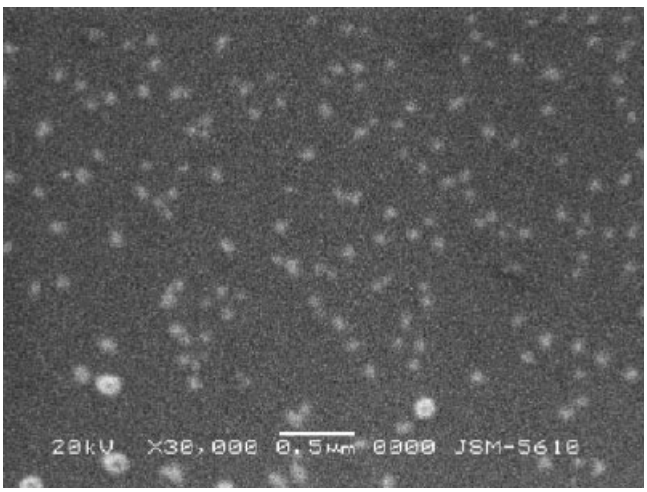

Figure 4 SEM micrograph of the SiO_2 clusters before being added to the cyanate ester.

Morphology of the BADCy/TMOS nanocomposites

In this study, the SiO_2 nanoparticles were generated via the sol–gel process, involving hydrolysis and condensation of a metal alkoxide precursor (TMOS). The particle size of the SiO_2 cluster depends on the conditions of the sol–gel process, which were previously described in the section on Preparation of Cyanate ester/SiO_2 Hybrids. Figure 4 shows the SEM micrograph of the SiO_2 clusters before being added to the cyanate ester. It was observed that the particle size of the silica clusters is about 30–50 nm, conforming to the value determined by the particle size analyzer (not shown here for brevity). Figures 5(a–c) are the SEM micrographs of the fracture surfaces of the completely cured hybrids for the samples T5, T10, and T20, respectively. The particle size observed in sample T5 [Fig. 5(a)] is in the range of 50–95 nm, which gradually increases with the increase of TMOS content, as shown in Figure 5(b,c) (10 phr and 20 phr TMOS). Meanwhile, the amount of silica clusters apparently increased with an increase of TMOS content. On the other side, the particle sizes in the cured hybrids (50–105 nm) were apparently magnified, when compared with those before being added to the cyanate ester (30–50 nm, as shown in Fig. 4). This fact is supposedly attributed to the further condensation of the silica cluster (POSS) during the cure reaction.

Physical properties of the BADCy/TMOS nanocomposites

Physical properties including the thermal degradation temperature, the glass transition temperature, the storage modulus, and the dielectric constant were thoroughly investigated by means of TGA, DMA, and impedance analyzer. All of these measurements are previously described in the section on Instrumentation, and all of the measured values are summarized in Table I.

Shown in Figure 6 are the typical TGA measurements of the cured cyanate ester/SiO_2 hybrids for samples of T5, T10, and T20, illustrating the thermal stability (thermal degradation temperature) and the char content. The thermal degradation temperature ($T_{d5\%}$) is defined as the temperature at which the weight loss is 5%. All of the $T_{d5\%}$ values (summarized in Table I) are higher than that of the neat BADCy network. But the values of $T_{d5\%}$ gradually increase with increasing silica content of the hybrid resins. Weights of residual char are markedly higher

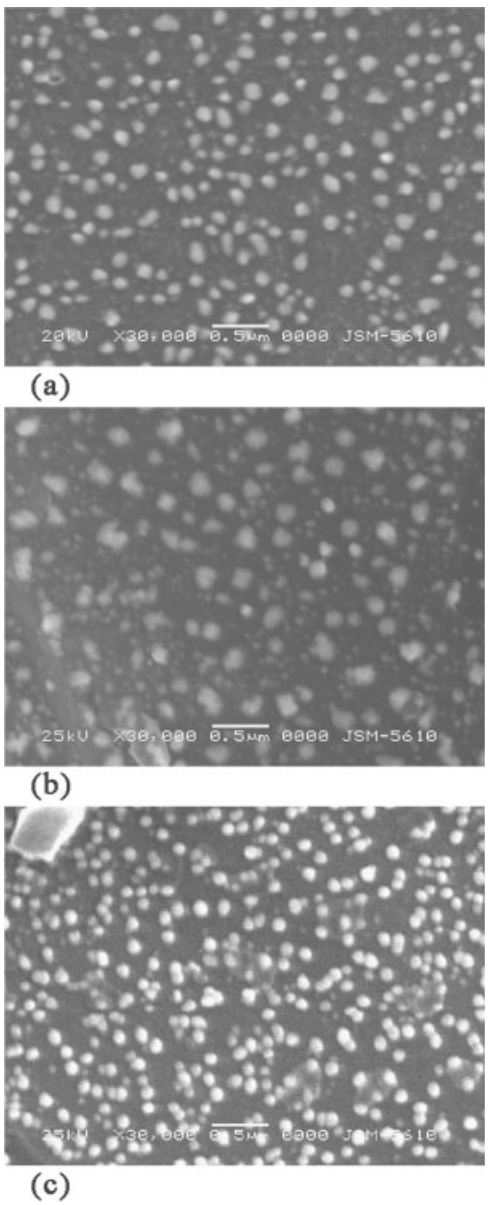

Figure 5 SEM micrographs of the fracture surfaces of the completely cured hybrids for the samples (a) T5, (b) T10, and (c) T20.

TABLE I
Physical Properties of the Cyanate Ester/SiO_2 Nanocomposites

Sample code	TMOS (phr)	ECOS (phr)	GPOS (phr)	SiO_2 (wt %)[a]	TGA (°C)[b] ($T_{d5\%}$)	T_g[c] (°C)	E′[d] (GPa)	Dielectric constant (D_k)[e] 1 GHz	1.8 GHz
BADCy (cured)	0	0	0	0	401	306	1.85	2.58	2.54
T5	5	0	0	2.18	419	296	2.12	2.47	2.31
T10	10	0	0	4.24	423	290	2.20	2.25	2.18
T20	20	0	0	8.06	424	285	2.25	2.03	1.95
E5	0	5	0	1.19	429	307	2.33	2.23	2.11
E10	0	10	0	2.29	395	290	1.75	2.24	2.08
E20	0	20	0	4.25	385	285	1.25	2.19	1.95
G5	0	0	5	1.24	414	305	1.73	2.30	2.20
G10	0	0	10	2.39	393	300	1.58	2.24	2.15
G20	0	0	20	4.44	383	285	1.28	2.27	1.98
T5E5	5	5	0	3.25	424	296	2.24	2.32	2.21
T5E10	5	10	0	4.25	406	285	1.97	2.30	2.20
T5G5	5	0	5	3.30	429	297	1.93	2.35	2.20
T5G10	5	0	10	4.35	402	284	1.78	2.31	2.19

[a] The silica contents were calculated by assuming that the sol–gel reactions proceed completely.
[b] The thermal degradation temperature ($T_{d5\%}$) is defined as weight loss 5 wt % in N_2, and is measured by TGA.
[c] The glass transition temperatures (T_g) were determined from the peak temperature of tan δ curve in the dynamic DMA runs.
[d] Values of storage modulus are defined as those at temperature of 50°C in the dynamic DMA runs.
[e] The dielectric constants (D_k) were determined with a HP4291B at frequency of 1 GHz and 1.8 GHz.

than the calculated values of silica content. The storage moduli (E') and tan δ were recorded via dynamic DMA runs (not shown for brevity). The glass transition temperature (T_g) is defined as the peak temperature of tan δ curve. For convenience, the storage moduli (E') listed in Table I were recorded at a temperature of 50°C. The glass transition temperatures (T_g's) in the nanocomposites showed only slightly smaller values than those in the neat BADCy system and exhibited a slight decrease with an increase of the silica content of the hybrid resins, mainly due to the increase of the free volume in the hybrid resulting from the presence of the silica cluster. On the contrary, the storage moduli (E') showed moderate increase with an increase in the silica content, because the silica clusters can act as fillers. Regarding dielectric constant, a trend of decreasing dielectric constant with increased silica content exists that is due to the increase of the free volume in the hybrid and the intrinsic property of POSS. POSS is usually used as an agent to lower the dielectric constant because of its high porosity.

BADCy/coupling agent systems

A coupling agent has been widely used to improve the compatibility between the two phases for preparation of the organic/inorganic nanocomposites via the sol–gel method.[4,5,10,11] Because the coupling agents were simultaneously composed of the epoxide groups and alkoxysilyl groups, some interactions between the polymer and the inorganic phases occur, and hence the inorganic cluster is tethered to the polymer main chain.

Characterization of the hybrid in the cure reactions

The cure reactions of liquid aromatic dicyanate ester with different types of epoxy resins (glycidyl ether type and cycloaliphatic oxide type) were investigated.[29] Similar chemical structures of the epoxide groups with those previously studied were used in this work. GPOS is a coupling agent with a glycidyl ether group, and ECOS contains a cycloaliphatic oxide group. In addition, the other end of GPOS and

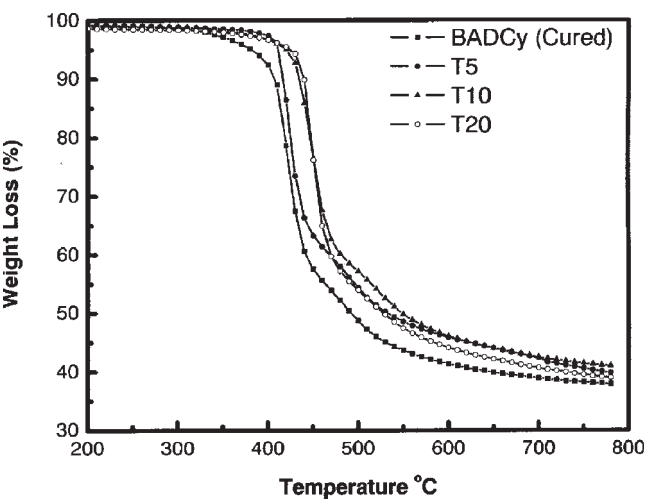

Figure 6 TGA measurements of the cured cyanate ester/SiO_2 hybrids for samples of T5, T10, and T20.

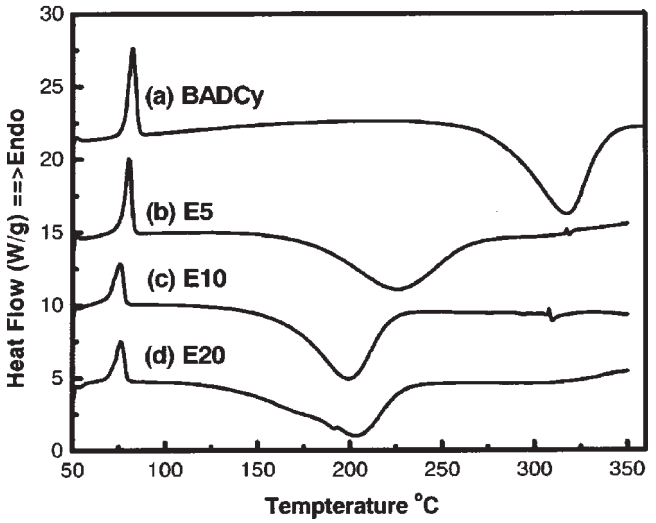

Figure 7 DSC thermograms at a heating rate of 20°C/min; (a) neat BADCy, (b) with 5 phr ECOS (E5), (c) with 10 phr ECOS (E10), and (d) with 20 phr ECOS (E20).

ECOS molecules were tethered with alkoxysilyl groups, which are the source of POSS.

The sol–gel process was carried out by virtue of hydrolysis and condensation of ECOS and GPOS, as previously described. Nanocomposites of the BADCy/ECOS hybrid or BADCy/GPOS hybrid were subsequently fabricated. Cure reactions of nanocomposites of the BADCy/ECOS hybrid or the BADCy/GPOS hybrid were investigated through a cross-reference between FTIR spectra and DSC thermograms. Shown in Figures 7(a–d) are the DSC thermograms of curing the BADCy hybrid associated with different levels of ECOS content (0, 5, 10, and 20 phr), respectively. In the presence of the ECOS component, only one exothermic peak exists, which dramatically shifts to a much lower temperature, when compared with neat BADCy [Fig. 7(a)], suggesting that the BADCy component reacts with the ECOS component and/or the BADCy component, which was catalyzed to undergo a polycyclotrimerization in the presence of residual acid and hydrolyzed —OH groups in the hybrid during the cure reaction. In addition, further condensation of POSS may also have occurred. Similarly, shown in Figures 8(a–d) are the DSC thermograms of curing the BADCy hybrid associated with different levels of GPOS content (0, 5, 10, and 20 phr), respectively. Interpretation of the reactions for the BADCy/GPOS hybrid is the same as those for the BADCy/ECOS hybrid. Shifts to a lower temperature of the BADCy/GPOS hybrids were less pronounced than those of the BADCy/ECOS hybrids, implying that GPOS accelerated the cure reaction less effectively than ECOS did.

The corresponding FTIR spectra for the cured BADCy/ECOS hybrids are shown in Figures 9(d–f), respectively. Curves (a)–(c) are for comparison. For all the cured samples (E5, 5 phr ECOS; E10, 10 phr ECOS; E20, 20 phr ECOS), the FTIR spectra show the consumption of most cyanate and epoxide groups. Simultaneously, concomitant reactions including the formation of triazine rings, oxazoline linkages, and POSS structures were also observed. The occurrence of these reactions can be verified by observing the following phenomena: (a) disappearing absorption bands of the cyanate group (2267 and 2237 cm^{-1}) and epoxide group (914 cm^{-1}), (b) emerging absorption bands of triazine (1565 and 1366 cm^{-1}) and oxazoline structure (1678 cm^{-1}), and (c) formation of POSS structure (the broadened Si—O—Si absorption bands at 1123 and 1026 cm^{-1}). The formation of triazine rings resulted from the polycyclotrimerization of BADCy, and oxazoline linkages were formed from the reaction of cyanate groups on the BADCy molecules with the epoxide groups on the ECOS molecules. This BADCy/ECOS hybrid underwent two reactions, illustrated as Path 1 and 3 in Scheme 1. In addition, the POSS structures were generated from the hydrolysis and condensation of alkoxysilyl groups on the end of ECOS molecules. The broadened Si—O—Si absorption bands at 1123 and 1026 cm^{-1} can be assigned to the cage and network structures of the POSS,[30,31] respectively. Collectively, these results revealed that the ECOS molecules were capable of forming covalent bonds between the cyanate esters and SiO_2 phases.

FTIR spectra for the cured BADCy/GPOS hybrids were shown in Figures 10(d–f), respectively. All reactions occurring in the BADCy/ECOS hybrid also took place in the BADCy/GPOS hybrid. This BADCy/GPOS hybrid underwent two reactions, illustrated as Path 1 and 2 in Scheme 1.

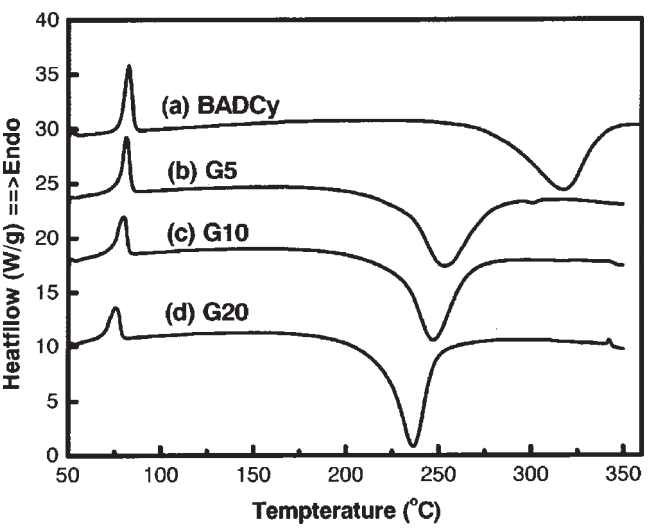

Figure 8 DSC thermograms at a heating rate of 20°C/min; (a) neat BADCy, (b) with 5 phr GPOS (G5), (c) with 10 phr GPOS (G10), and (d) with 20 phr GPOS (G20).

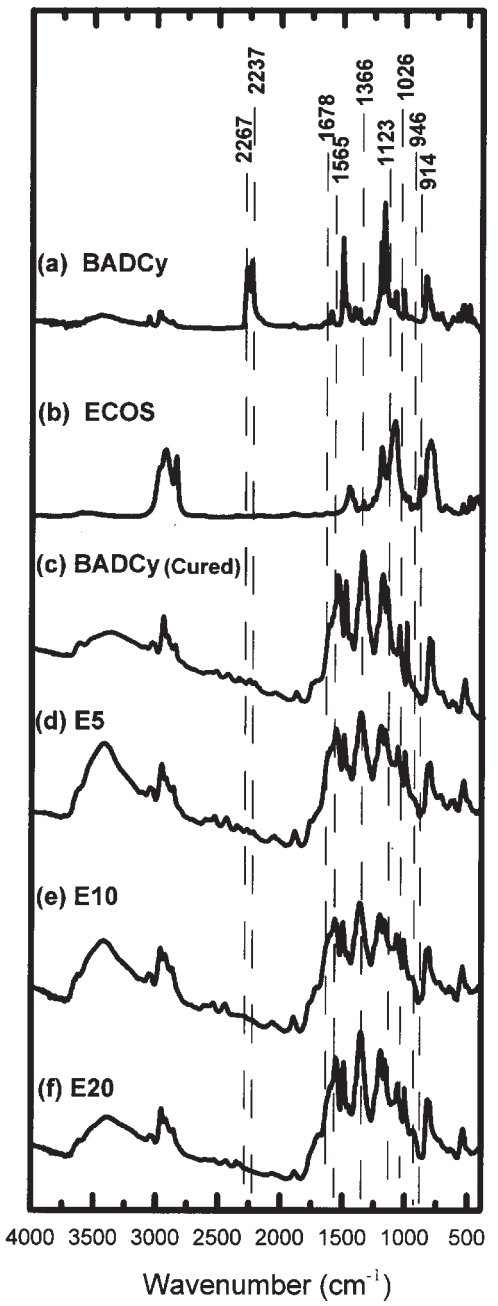

Figure 9 FTIR spectra for (a) neat BADCy monomer, (b) pristine ECOS, (c) cured BADCy, (d) cured E5 (with 5 phr ECOS), (e) cured E10 (with 10 phr ECOS), and (f) cured E20 (with 20 phr ECOS).

A representative solid-state ^{29}Si NMR spectrum was shown in Figure 3(b), displaying the cured nanocomposite sample E20 (20 phr ECOS). Chemical shifts of −57 and −66 ppm were detected and assigned to T^2 and T^3, respectively. All samples (E5, E10, E20, G5, G10, and G20) showed that T^3 was the predominant microstructure, revealing that most of the alkoxysilyl groups formed network or cage structures—results that were similar with those for the BADCy/TMOS nanocomposites.

Morphology of the BADCy/coupling agent nanocomposites

The SiO_2 nanoparticles were generated from the hydrolysis and condensation of alkoxysilyl groups on the end of the coupling agents (ECOS or GPOS) via the sol–gel process. The particle size of the SiO_2 clusters before being added to the cyanate ester was in the range of 10–30 nm (not shown here for brevity). It was apparently smaller than those in the TMOS systems (30–50 nm), probably due to the fact that

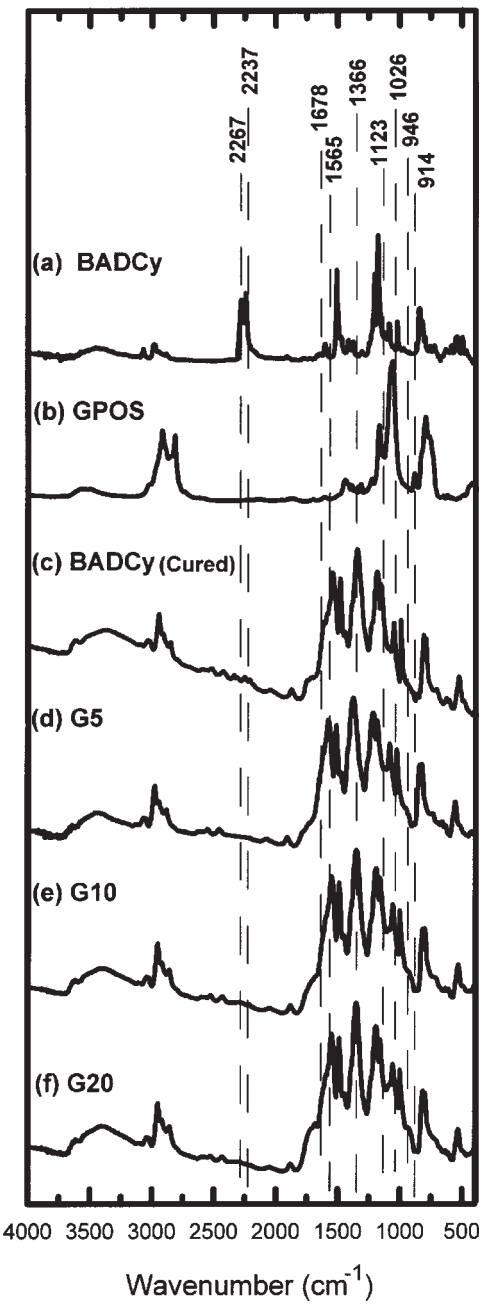

Figure 10 FTIR spectra for (a) neat BADCy monomer, (b) pristine GPOS, (c) cured BADCy, (d) cured G5 (with 5 phr GPOS), (e) cured G10 (with 10 phr GPOS), (f) cured G20 (with 20 phr GPOS).

the alkyl chain in the coupling agents (ECOS or GPOS) hindered the condensation of the alkoxysilyl groups to form POSS clusters. Steric hindrance effects obviously increased as the condensation of POSS cluster continuously proceeded, and hence the number of alkyl chains bonded to the POSS cluster increased. That is why the silica clusters maintained a smaller size. Figures 11(a–c) are the SEM micrographs of the fracture surfaces of the completely cured hybrids for the samples E5, E10, and E20, respectively. The amount of silica clusters apparently increased with the increase in the ECOS content, but the particle sizes seemed unaltered and were in the range of 30–50 nm. These sizes were slightly magnified, when compared with those before being added to the cyanate ester (10–30 nm). This fact is supposedly attributed to the further condensation of the silica cluster (POSS) during the cure reaction, but is still subject to the steric hindrance effect of the alkyl chains around the silica cluster. Nevertheless, the particle sizes of the cured hybrid in this system did not increase with an increase of ECOS content and were much smaller than those in the BADCy/TMOS system (50–105 nm), which can be mainly attributed to the covalent bonding of ECOS with BADCy. The silica clusters were thus dragged away and were homogenously separated and tethered to the BADCy network.

The phenomena in the BADCy/ECOS hybrids were also observed in the BADCy/GPOS hybrids. In the BADCy/GPOS system, the amount of silica clusters apparently increased with an increase of GPOS content, but the particle sizes remained unaltered, compared with those in the BADCy/ECOS system, and were also homogenously separated in the particle size range of 30–50 nm.

Physical properties of the BADCy/coupling agent nanocomposite

The physical properties of the BADCy/coupling agent nanocomposites are summarized in Table I. Despite the fact that the silica content increased with increasing coupling-agent contents in the hybrid resins, the values of $T_{d5\%}$, T_g and the storage moduli (E') either in the BADCy/ECOS hybrids or in the BADCy/GPOS hybrids gradually decreased when increasing the coupling agent content. For the same content of metal alkoxide precursors (such as E5 vs. T5, or E10 vs. T10, etc.), all the samples in the BADCy/coupling agent always exhibited inferior mechanical properties and thermal stability than those in the BADCy/TMOS hybrids. Nevertheless, the values of $T_{d5\%}$ in the samples containing 5 phr coupling agent were still higher than those in the neat BADCy network. The main reasons for this are supposed as follows: (1) the increase of the free

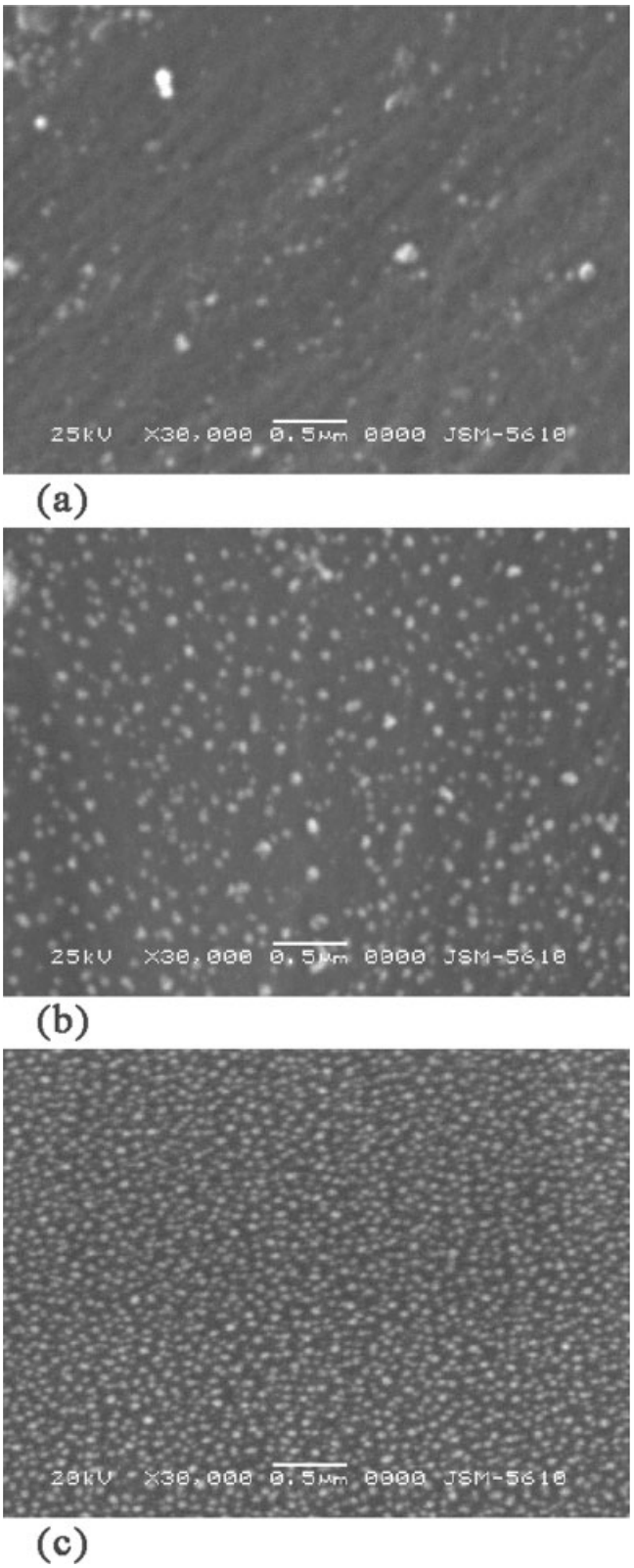

Figure 11 SEM micrographs of the fracture surfaces of the completely cured hybrids for the samples (a) E5, (b) E10, and (c) E20.

volume in the hybrid, (2) the presence of ether linkages in the coupling agent and hence in the hybrids, (3) the decrease of crosslink density resulting from the addition of coupling agents which participated in the reaction with cyanate groups on the BADCy monomer.

For the BADCy/coupling agent nanocomposites, a trend of decreasing dielectric constant with increased silica content exists, which is virtually the same as in the BADCy/TMOS nanocomposites. A higher POSS content leads to higher porosity and larger free volume in the hybrid.

BADCy/TMOS/coupling agent system

The characterization of the BADCy/TMOS nanocomposites shows improved physical properties and a slightly larger particle size with increased silica content. On the other hand, the characterization of the BADCy/coupling agent nanocomposites illustrated weakened physical properties but are of smaller and homogenous particle sizes, irrespective of the silica content. Therefore, the BADCy/TMOS/coupling agent system was designed to combine the advantages of the two systems as mentioned earlier.

The preparation method of this system was somewhat different from the one in the BADCy/TMOS and BADCy/coupling agent systems. To avoid reactivity discrepancies between TMOS and the coupling agents, the two components were separately dissolved in different solutions. The coupling agent (GPOS or ECOS) was dissolved in THF solvent together with BADCy rather than with TMOS, and it is referred to as Solution A, whereas Solution B was composed of TMOS/H_2O/HCl/THF in a specified mole ratio. The sol–gel process was carried out first for Solution B to produce the isolated nanoparticles, as previously described in the Preparation of Cyanate ester/SiO_2 Hybrids section. Subsequently, Solutions A and B were thoroughly mixed and stirred for another hour to further hydrolysis and condensation reactions. The subsequent procedures were virtually the same as previously described. The BADCy/TMOS/coupling agent nanocomposites were thus fabricated. Some formulations were designed, such as samples of T5E5, T5E10, T5G5, and T5G10, and these compositions are listed in Table I, respectively.

The microstructure was demonstrated to be a highly crosslinked nanocomposite composed of isolated SiO_2 clusters and tethered SiO_2 clusters, including the following aspects. (1) One end of the coupling agent underwent reactions with BADCy to form an oxazoline structure, while the other end of the coupling agent was capable of forming SiO_2 clusters. (2) The isolated particles of the SiO_2 clusters were generated from the TMOS component. The nanoparticles were homogenously distributed in the hybrid, and the particle sizes were in the range of 30–80 nm. The part of smaller particle sizes is supposedly attributed to the coupling agents, whereas the part of larger particle sizes resulted mainly from the TMOS component. The particle sizes could be controlled by adding different amounts of TMOS component.

Physical properties in the BADCy/TMOS/coupling agent nanocomposites are summarized in Table I. The glass transition temperatures (T_g's) in those nanocomposites showed only slightly lower values than that in the neat BADCy system. Nevertheless, all the values of storage moduli (E'; except for T5G10) and $T_{d5\%}$ were superior to those in the neat BADCy network. The values of $T_{d5\%}$, T_g, and storage moduli (E') in the nanocomposites gradually decreased with increasing SiO_2 content. The dielectric constants of those nanocomposites were also reduced.

CONCLUSIONS

It is believed that introducing inorganic particles into a polymer matrix can enhance the thermal stability and mechanical properties of the resulting composites, particularly when introducing nanoparticles. BADCy/TMOS nanocomposites containing isolated silica nanoparticles were produced as expected. It can be inferred that the use of coupling agents improves some of the physical properties, because the coupling agent strengthens the bonding between the organic polymer matrix and the inorganic particles. Unfortunately, the coupling agents (GPOS and ECOS), which were used in this study, did not result in the desired target. Although oxazoline linkages were generated to form covalent bonds between the cyanate esters and the coupling agents, and silica clusters were simultaneously tethered to the matrix, the desired preferable physical properties could not be achieved probably due to the presence of ether linkages and longer soft chains in the coupling agent, and hence in the BADCy/coupling agent hybrids. However, the BADCy/TMOS/coupling agent system was successfully designed to combine the advantages of the two mentioned systems.

In the highly crosslinked BADCy/TMOS hybrid system, the particle sizes can be controlled within the range of 50–105 nm by adding different amounts of TMOS. In the highly crosslinked BADCy/coupling agent hybrid system, the particle sizes were kept small in the range of 30–50 nm, irrespective of the amounts of coupling agent added. The BADCy/TMOS/coupling agent hybrid system simultaneously possessed both isolated and tethered silica clusters in the range of 30–80 nm. Steric hindrance effects of alkyl chains on the coupling agent obviously played an important role in the later two cases.

Although the thermal property ($T_{d5\%}$) and the mechanical property (E') in the BADCy/coupling agent hybrid system showed weakened values, extra addition of the TMOS component in those hybrids (i.e., BADCy/TMOS/coupling agent hybrid) could improve $T_{d5\%}$ and E' to some extent. Even for the samples T5E10 and T5G10, the $T_{d5\%}$ and E' values were still higher than those in the neat BADCy network.

All the glass transition temperatures (T_g's) in the nanocomposites showed only a slightly lower value than that in the neat BADCy system, supposedly attributed to the increase of the free volume resulting from the formation of silica clusters. On the other hand, all the dielectric constants in the nanocomposites were significantly reduced, probably due to the increase of the free volume in the hybrid and the vast porosity of poly(silsesquioxanes).

References

1. Wen, J.; Wilkes, G. L. Chem Mater 1996, 8, 1667.
2. Hsiue, G. H.; Kuo, W. J.; Huang, Y. P.; Jeng, R. J. Polymer 2000, 41, 2813.
3. Chen, Y.; Iroh, J. O. Chem Mater 1999, 11, 1218.
4. Kioul, A.; Mascia, L. J Non-Cryst Solids 1994, 175, 169.
5. Shang, X. Y.; Zhu, Z. K.; Yin, J.; Ma, X. D. Chem Mater 2002, 14, 71.
6. Yen, C. T.; Chen, W. C.; Liaw, D. J.; Lu, H. Y. Polymer 2003, 44, 7079.
7. Morrikawa, A.; Yamaguchi, H.; Kakimoto, M. A.; Imai, Y. Chem Mater 1994, 6, 913.
8. Wang, S.; Ahmad, Z.; Mark, J. E. Chem Mater 1994, 6, 943.
9. Chen, W. C.; Lee, S. J. Polym J 2000, 32, 67.
10. Huang, Z. H.; Qiu, K. Y. Polym Bull 1995, 35, 607.
11. Huang, Z. H.; Qiu, K. Y. Polymer 1997, 38, 521.
12. Landry, C. J. T.; Coltrain, B. K. Polymer 1992, 33, 1486.
13. Noell, J. L. W.; Wilkes, G. L.; Mohanty, D. K.; McCrath, J. E. J Appl Polym Sci 1990, 40, 1177.
14. Chiang, P. C.; Whang, W. T. Polymer 2003, 44, 2249.
15. Qiu, W.; Luo, Y.; Chen, F.; Duo, Y.; Tan, H. Polymer 2003, 44, 5821.
16. Mauritz, K. A. Mater Sci Eng C 1998, 6, 121.
17. Chiang, C. L.; Ma, C. C. M. Eur Polym J 2002, 38, 2219.
18. Liu, Y. L.; Hsu, C. Y.; Wei, W. L.; Jeng, R. J. Polymer 2003, 44, 5159.
19. Ochi, M.; Takahashi, R.; Terauchi, A. Polymer 2001, 42, 5151.
20. Kang, S.; Hong, S. I.; Choe, C. R.; Park, M.; Rim, S.; Kim, J. Polymer 2001, 42, 879.
21. Ramirez, M. L.; Walters, R.; Lyon, R. E.; Savitski, E. P. Polym Degrad Stab 2002, 78, 73.
22. Lin, R. H.; Hong, J. H.; Su, A. C. Polymer 1995, 36, 3349.
23. Hong, J. H.; Wang, C. K.; Lin, R. H. J Appl Polym Sci 1994, 53, 105.
24. Lin, R. H.; Hong, J. H.; Su, A. C. J Polym Res 1997, 4, 191.
25. Lin, R. H.; Hong, J. H.; Su, A. C. J Polym Sci Part B: Polym Phys 2000, 38, 726.
26. Lin, R. H.; Hong, J. H.; Su, A. C. Polym Int 2000, 49, 345.
27. Lin, R. H.; Lu, W. H.; Lin, C. W. Polymer 2004, 45, 4423.
28. Lin, R. H.; Lee, W. H.; Lu, A. C.; Lin, C. W. J Appl Polym Sci 2004, 94, 345.
29. Lin, R. H. J Polym Sci Part A: Polym Chem 2000, 38, 2934.
30. Lee, L. H.; Chen, W. C.; Liu, W. C. J Polym Sci Part A: Polym Chem 2002, 40, 1560.
31. Liu, W. C.; Yang, C. C.; Chen, W. C.; Dai, B. T.; Tsai, M. S. J Non-Cryst Solids 2002, 311, 233.